Polym. Bull. (2009) 62:225–235
DOI 10.1007/s00289-008-0005-z

ORIGINAL PAPER

Formation of dendrite crystals in poly(ethylene oxide) interacting with bioresourceful tannin

Kai Cheng Yen · E. M. Woo

Received: 27 August 2008 / Revised: 17 October 2008 / Accepted: 8 November 2008 /
Published online: 25 November 2008

Abstract A dendritic morphology, induced by miscibility with strong intermolecular interaction between poly(ethylene oxide) (PEO) and bioresourceful tannin [tannic acid (TA)]. Mechanism was investigated by differential scanning calorimetry (DSC), Fourier-transform infrared spectroscopy, wide-angle X-ray diffraction, and polarized optical microscopy. The cell crystallography preference in correlation to the intermolecular interaction in the dendrites in PEO/TA (70/30) blend was analyzed. Dendritic morphology was more distinct at PEO/TA = 70/30 composition, where the spherulitic growth rate showed a highly nonlinear relationship with respect to crystallization time ($R \propto t^{1/2}$). Diffusion limitation mechanism caused by the crystallography preference attributed to the strong intermolecular interaction between PEO and TA was at work.

Keywords Poly(ethylene oxide) · Dendrite

Introduction

Subjects on spherulitic morphology of semicrystalline polymers have attracted much attention in the past few years. There are many complex factors that determine the spherulitic morphologies, such as crystallization temperature, composition of amorphous polymer, thermal treatment and intermolecular interaction, etc. The spherulitic morphologies and crystallization kinetics in PEO and PEO/amorphous polymer blends have been studied in past decades [1–5]. For PEO/amorphous polymer blends, the spherulite morphologies are quite different among those blends with or without strong intermolecular interactions [6–12]. PEO/poly(*n*-buytyl methacrylate) (PnBMA) [6], PEO/poly(vinyl acetate) (PVAc) [7], PEO/poly(methyl

K. C. Yen · E. M. Woo (✉)
Department of Chemical Engineering, National Cheng Kung University, Tainan 701-01, Taiwan
e-mail: emwoo@mail.ncku.edu.tw

methacrylate) (PMMA) [7] and PEO/poly(vinyl chloride) (PVC) [8] are miscible blends with weak intermolecular interactions, and their crystalline morphologies are of normal Maltese-cross pattern which is the same as neat PEO. In contrast, for miscible blends with strong intermolecular interactions, like PEO/styrene-hydroxystyrene copolymer (SHS) [7], PEO/poly(*p*-vinyl phenol) (PVPh) [9], PEO/4,4'-diaminodiphenylsulfone (DDS) [9, 10], PEO/unsaturated polyester resin (PER) [11] and PEO/hydroquinine [12], the spherulite morphologies in these blends become feather-like or dendritic with increasing contents of the amorphous polymer in blends.

Dendritic morphologies can occur in ultra-thin film PEO (50–100 nm) by Reiter et al. [13–15], who have pointed out that growth of the crystallites into two-dimensional finger-like patterns can start from the rim of de-wetted regions. The crystallites are built up from molecular stems which are oriented upright with respect to the surface and the surface fraction of the finger structures in the de-wetted regions after crystallization can be directly related to the average length of the stems or to the average number of stems per chain. During growth, the remaining part of the monolayer thin film gets more and more diluted, thus the crystal growth becomes finally diffusion controlled, resulting in a fingerlike morphology. The chains are therefore frustrated under steady-state conditions, thus forming a non-equilibrium structure with respect to both two-dimensional geometry (fractal or fingerlike patterns) and internal ordering (average stem length) [13–15].

In this study, instead of restriction of ultra-thin films and de-wetting environment provided by ultra-thin films, effects of diluents specifically interacting with PEO were probed. In this study, focus was placed on dendritic morphology and its comparative mechanism in PEO/amorphous polymer blends with strong intermolecular interactions between the two components. Although peculiar dendritic morphology has been reported for PEO blended amorphous polymers, mechanism is not completely clear. In addition, blends of PEO with bio-resourceful polymers (or diluents) have been less studied. A bioresourceful and biocompatible tannin, with polyphenol groups, was chosen as an ideal model for blending with PEO in probing effects of tannin's strong hydrogen bonding interactions on PEO crystalline morphology. The phase behavior and the mechanism of dendrites formation in PEO/tannin blends were probed.

Experimental

Materials

Semicrystalline poly(ethylene oxide) (PEO) was purchased from Aldrich, with $M_w = 200{,}000$ g mol^{-1}, $T_m = 60$ °C and $T_g = -60$ °C. Tannin [or tannic acid (TA)], a natural derivative from tea with MW = 1,721 g/mol, was obtained from Sigma-Aldrich Co. (USA) and was used without further purification. Structure of TA is shown in Scheme 1, which shows TA is a macromolecular aromatic ester with two to three –OH groups on each of 10 benzene rings.

The polymers were first weighed, respectively, and dissolved into *p*-dioxane solvent (4 wt% polymers) with continuous stirring with a magnetic bar. HPLC-

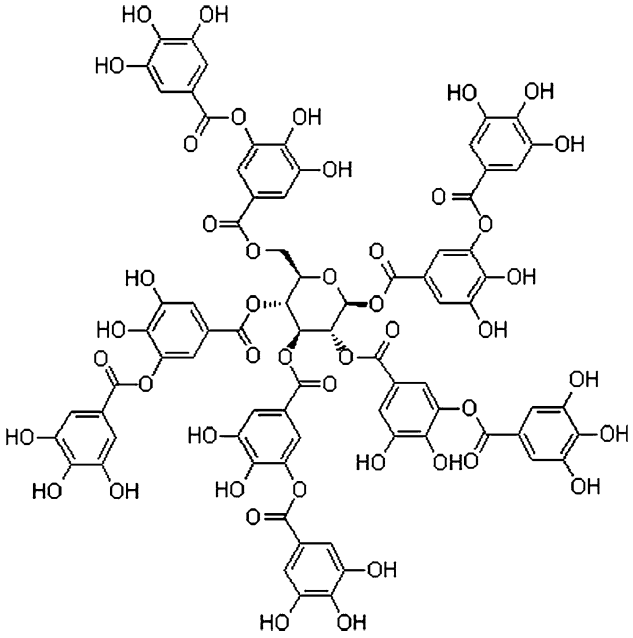

Scheme 1 Tannic acid (Tannin)

grade solvent was used for blend preparation. Subsequently, proper quantity of the resulting polymer solution was poured into a flat aluminum or glass mold at room temperature. For polarized optical microscopy (POM) characterization, polymer solution was spread/cast on micro glass slides and dried. All solution-cast blend samples were initially air dried and finally subjected to a vacuum oven at 40 °C for 7 days to ensure complete removal of residual solvent. The film thickness was ca. 20 μm, which was considered to be thin but not ultra-thin.

Apparatus

Wide-angle X-ray diffraction (WAXD) analysis was performed using a Shimadzu XRD-6000 with copper K_α radiation (30 kV and 40 mA) and a wavelength of 1.542Å. The scanning 2θ angle range was from 5° to 35° with a step of 0.02° or equivalent to scanning rate of 2 min^{-1}. X-ray samples were prepared by casting the polymer solution on a polyimide (PI) film and the film thickness was ca. 20 μm.

The melting behavior was investigated using a differential scanning calorimetry-7 (DSC-7) (Perkin-Elmer). The temperature and heat of transition of the instrument were calibrated with indium and zinc standards. To determine the thermal behaviors of PEO/TA blends, a dynamic heating rate of 20 °C min^{-1} was used. During thermal annealing or scanning, a continuous nitrogen flow in the DSC sample cell was maintained to ensure minimal sample degradation. In addition, the DSC cells were also used for precisely controlling the thermal treatments of the samples.

Crystal morphology was observed using Nikon Optiphot-2 POM, charge-coupled device (CCD) digital camera, and a Linkam THMS-6000 microscopic heating stage with TP-92 temperature programmer. The CCD equipped with automated image software was used to capture the morphology of the isothermally crystallized samples at preset time intervals. Thin films of the specimens for POM were sandwiched between two glass slides. These samples were first melted on the hot stage at 100 °C for 5 min to completely remove prior thermal history of the blends and then were quickly quenched to a designated temperature T_c for isothermal crystallization.

Fourier-transform infrared spectroscopy (FTIR, Nicolet Magna-560) was used for investigating possible molecular interactions between the constituents. Spectra were obtained at 4 cm^{-1} resolution and averages of spectra were obtained from at least 64 scans (for enhanced signal) in the standard wavenumber range 400–4,000 cm^{-1}. Blend samples for IR measurements were cast as thin films with uniform thickness directly on KBr pellets at ambient temperature. Subsequently, IR measurements were performed on the samples cast on KBr pellets.

Results and discussion

The cast-films of PEO/TA blends from *p*-dioxane were examined through POM in all composition range at ambient temperature and then above the melting temperature of polyesters (70–80 °C). The results indicated that the blend films up to 40 wt% of TA were all optically clear without any phase heterogeneity. But the films containing less than 40 wt% of TA showed some textures because of crystalline polyester phase at ambient temperature. However, these films were found to be optically clear and homogeneous when heated above the melting temperatures. The OM graphic results of phase homogeneity above T_m are not shown here for brevity.

The crystalline morphologies of neat PEO and PEO/TA blends crystallized at $T_c = 30$ °C after quenching from melt were observed by POM and shown in Fig. 1a–c).

Figure 1a shows typical spherulites with normal Maltese-cross extinction patterns in fully crystallized PEO. However, in blending with TA, the crystalline morphologies of PEO in the PEO/TA blends change with the TA content. Figure 1b shows the spherulite morphology of PEO/TA = 80/20, where the spherulite

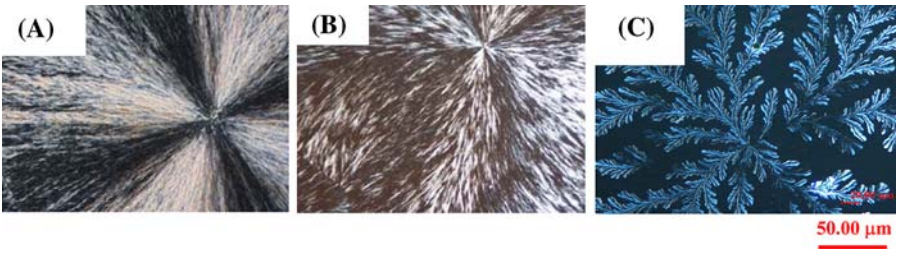

Fig. 1 Spherulite morphologies for **a** neat PEO, **b** PEO/TA = 80/20, and **c** PEO/TA = 70/30, all melt-crystallized at 30 °C

becomes less compact and differs significantly from that of neat PEO. Besides, the growth of the spherulite of PEO in PEO/TA = 80/20 is no longer along the radial direction but in a curved direction. Further increase the TA content to 30 wt%, the crystalline morphology of PEO/TA = 70/30 shown in Fig. 1c becomes dendritic/feather-like and non-volume filling. Normally, the feather-like dendritic pattern is seen only in blends systems of PEO with strong-interacting species [7–12]. As the TA content was up to 40 wt%, the PEO chains in the PEO/TA blend became totally amorphous, and could not form any spherulite crystals in all range of temperatures investigated. Apparently, TA effectively depresses the crystallizing tendency of PEO owing to stronger interactions and the addition of TA causes great influences in the crystalline morphologies of PEO.

Effects of TA blending on the glass transition behavior in PEO/TA blends were investigated and analyzed by DSC. Figure 2 shows the DSC traces of PEO and PEO/TA blends scanned from −60 °C (amorphous glassy state), which is quenching from melt, to 80 °C (amorphous molten state) with scanning rate = 20 °C/min. In the thermal traces of neat PEO and PEO/TA = 80/20, T_g in the two traces was not easily observed because of the fully crystallization of PEO upon quenching and the amorphous polymer chains of PEO were few and restricted by the crystalline domains of PEO. For the other blend compositions (PEO/TA = 70/30, 60/40, 40/60, 20/80), there exists only a single T_g in each DSC trace, and the value of T_g increases with increase in the TA content. The single and composition-dependent T_g behavior shows that the PEO/TA blend system is miscible. The heat of fusion and the melting temperature of PEO decrease rapidly with the increase of TA in blends. Besides, the cold crystallization peak ($T_{c.c}$ as indicated in the DSC trace for PEO/TA = 70/30), which is not present in neat PEO or PEO/TA = 80/20, appears in the thermal trace of PEO/TA = 70/30, indicating that the crystallization of PEO upon quenching was retarded by TA. When TA content was up to 40 wt% or more in blends, there showed no endothermic peak in each trace upon DSC scanning, suggesting that the crystallinity of PEO was completely depressed. Consequently, it shows clear evidence for the effective depression in the crystallization rate and the crystallinity of PEO with the introduction of TA. The great influence and depression in the PEO crystallinity when blended with TA may be attributed to existence of the strong intermolecular interaction between PEO and TA.

Then, FT-IR method was used to verify the existence of the specific intermolecular interactions between PEO and TA components in the PEO/TA blends. Figure 3a shows the FT-IR spectra of hydroxyl-stretching region of PEO, TA, and their blends of different compositions. The spectrum for neat TA exhibits a broad band at 3,362 cm^{-1} along with a shoulder peak at 3,206 cm^{-1}, which can be attributed to stretching frequency of free –OH group and inter-associating hydroxyl groups of TA, respectively.

The free hydroxyl peak (3,362 cm^{-1}) vanishes with increasing PEO content in the blend to 40 wt%. It can be easily discerned that this band slowly shifts to a higher wavenumber and ultimately overlaps with the free hydroxyl-stretching peak. These changes are due to the breaking-up of H-bonded hydroxyl bond and the formation of new H-bond between the hydroxyl group of TA and ether group of PEO. Figure 3b shows FTIR spectra of the C–O–C region of PEO and its blend of

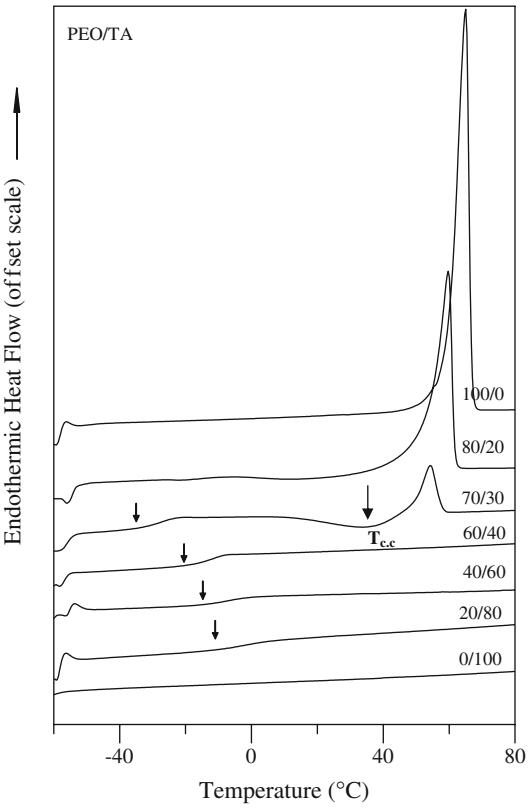

Fig. 2 DSC traces (20 °C/min) for quenched PEO/TA blends indicating single T_g

different compositions as indicated in the curve. The wavenumber of the C–O–C peak of PEO for the blend shifts from 1,112 to 1,101 cm^{-1} as the TA composition increases to 40 wt% and then merges with the absorption bands of TA with further the increase of the TA content. The down-shift apparently increases as the TA content in PEO/TA blend increases. This confirms the existence of hydrogen bonding between the ether group of PEO and hydroxyl group of TA in the PEO/TA blend. In addition, the CH_2 wagging mode was observed at $\sim$1,350 cm^{-1} in the blend composition of PEO/TA = 60/40, which split into two peaks at 1,342 and 1,359 cm^{-1} for the samples with PEO contents more than 80 wt%. The result reveals the presence of the crystalline phase of PEO in the PEO/TA blend with higher PEO content (higher than 80 wt%) and the PEO crystallizing tendency is suppressed with increase of TA contents in the PEO/TA blends, which is in good agreement with the results of DSC analysis.

For miscible polymer blends comprising a crystallizable component, the growth rate of the crystallizable component can be influenced by the amorphous diluent in blends. The change of the crystallization rate caused by diluents depends on the mutual interactions, relative difference in T_g values of the two components and the compositions of diluents, etc. Figure 4a is the plot of the spherulitic radius versus time for three compositions of PEO/TA blend (100/0, 80/20, and 70/30) observed by

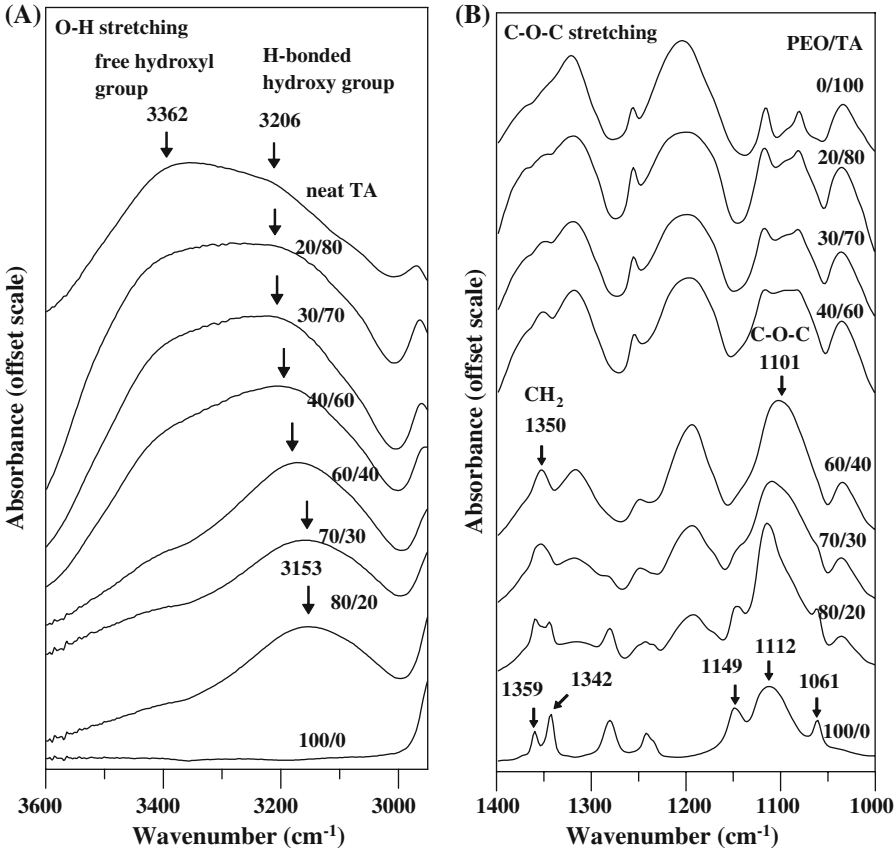

Fig. 3 FTIR spectra for **a** O–H, and **b** C–O–C stretching in PEO/TA blends of eight compositions

POM. The crystal growth rates of PEO in the blends decrease severely with the addition of TA, especially for PEO/TA = 70/30. Besides, the spherulite radii in neat PEO and PEO/TA = 80/20 show linear relationships with respect to time, but show a nonlinear relationship to time in PEO/TA = 70/30. It means that the spherulite growth rate (the slope) of PEO in PEO/TA = 70/30 is not a constant and decreases with time.

Effects of impurity or amorphous diluent segregation on the crystallization kinetics of semicrystalline polymers in polymer blends have been studied by Keith and Padden [16], and they have concluded that if the crystal growth rates of crystallizable polymers are higher than the diffusion rates of the impurity/amorphous diluents, the diluents are trapped in the interlamellar or interfibrillar regions. However, if the diffusion rates of the diluents are higher than the crystal growth rate of crystallizable polymers, it leads to the segregation of the amorphous diluents in the interspherulitic regions, and the concentration of the diluents at the crystal growth front increases. In this case of PEO/TA = 70/30, from observation of the non-volume filling dendritic morphology and the retardation of the crystal

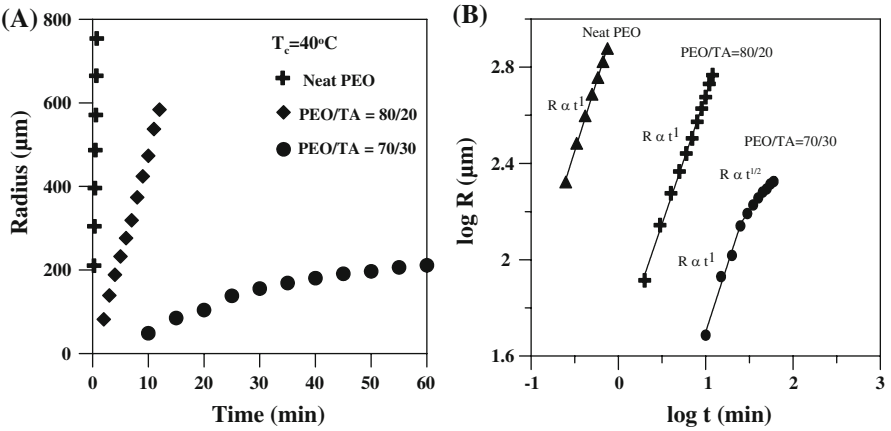

Fig. 4 **a** Plots of spherulites radii versus time, and **b** log R versus log t for PEO and PEO/TA blends melt-crystallized at 40 °C

growth rate with isothermal crystallization time by POM, the amorphous diluents (TA) may segregate in the interspherulitic region. It may be due to the lower crystal growth rate of PEO, which is caused by the strong intermolecular interactions with TA, compared with the diffusion rates of the amorphous diluents. These results explain that the formation of the unusual dendritic/feather-like morphology instead of spherulitic morphology with Maltese-cross extinction observed in neat PEO can be frequently obtained in PEO/amorphous polymer blend systems with strong intermolecular interactions. Data of growth rates of PEO and PEO/TA blends are plotted in Fig. 4b, where log R versus log t for neat PEO, and PEO/TA blends. Linear relationships obtained in PEO/TA = 100/0 and 80/20 indicate that the growth rates are constant. However, in PEO/TA = 70/30, the relationship of log R versus log t can be divided into two regions with different slopes, where in the shorter time region, the radius is proportional to time, i.e. $R \propto t^1$; but in the longer time region, the relationship of radius and time is in $R \propto t^{1/2}$. Wu et al. [7] have reported that the change in the correlation with radius and time from $R \propto t^1$ to $R \propto t^{1/2}$ indicates the change in growth mechanism to diffusion-limited mechanism. Thus, by similar interpretation, the dendritic morphology in the PEO/TA blend may be attributed to a diffusion-limited mechanism originating from strong interactions between the components.

Miscible blends comprising a semicrystalline polymer exhibit strong intermolecular interactions with the other component have been studied in the past decades, such as aliphatic polyesters/TA [17], poly(L-lactic acid) (PLLA)/PVPh [18], and poly(trimethylene terephthalate) (PTT)/PVPh [19], etc. However, dendritic morphologies are not always observed in systems with strong intermolecular interactions. The issue of dendritic morphology in polymers or blends may be interesting and worthy of investigations. The formation of the dendritic morphology is likely attributed to the diffusion-limited mechanism and the diffusion-limited mechanism occurs when the crystal growth rate is lower than the chain diffusion

rate. Thus, it is supposed that the extent of the intermolecular interaction in PEO/amorphous polymer blend is higher than that in other miscible blends with strong intermolecular interactions and leads to the slower crystal growth rate in PEO in blends. It is useful to compare with the relative absorbance of the free-hydroxyl band to the inter-associated hydroxyl band in the hydroxyl-stretching region of the PEO/TA blends in this study to that of PCL/TA blends discussed in previous literature result [17]. The intensities of the inter-associated hydroxyl band (3,206 cm^{-1}) in almost all compositions of PEO/TA blends are higher than those of the free hydroxyl band, while the intensities of the inter-associated hydroxyl band in almost all compositions of PCL/TA blends are lower than those of the free hydroxyl band. These comparisons show that the extent of the intermolecular interactions in PEO/TA blends is higher than that in PCL/TA blends. Hence, this provides further evidence that the dendritic morphology in PEO/amorphous polymer blends may be attributed to the strong intermolecular interaction in the amorphous liquid state. Such strong intermolecular interaction between TA and the crystallizing species also leads to some peculiar changes in intrinsic characteristic features of the crystal growth in PEO.

Thus, the analysis of the crystal growth in neat PEO and PEO/TA blends, the cast-films of PEO and PEO/TA blends were also investigated by WAXD to study the effect of strong intermolecular interactions on the crystallographic orientation of PEO. The polymer solutions of each blend composition were spread onto PI films and then degassed in vacuum oven for complete removal of the residual solvent. The thickness of the polymer film for each composition in PEO/TA or PEO/PVPh blends produced on PI film was ca. 20 μm. The crystalline morphologies in neat PEO and PEO/TA blends formed on PI films were firstly observed by POM and showed the same as that cast on glass slides shown earlier in Fig. 1. Additional POM characterization showed that the crystalline morphology in the PEO/PVPh = 70/30 blend revealing a similarly dendritic morphology, which was almost same as that for the PEO/TA = 70/30 blend. Detailed POM morphology for the PEO/PVPh blend is not shown here for brevity. Blends on PI films (7–10 pieces) were stacked up for sufficient signal intensity in WAXD analysis. Figure 5 shows the WAXD patterns of PEO, PEO/TA blend and PEO/PVPh blend cast on PI films at ambient temperature (28 °C). Four diffraction peaks corresponding to (120), (032), (024) and (131) planes are present from low to high diffraction angles. The peak positions do not change in different blend compositions, which indicate that the d-spacing of the crystal planes of PEO is not disrupted by the hydrogen bonding. Figure 5a shows that the intensity of the (032) crystal plane is higher than that of the (120) crystal plane in neat PEO crystallized at 28 °C. However, for PEO/TA = 80/20 and 70/30 blends as shown in Fig. 5b, c, the intensities of (032) crystal plane become lower than that of (120) crystal plane, indicating that the introduction of TA content may cause the difference in the crystallographic orientation for the formation of the strong intermolecular interactions between PEO and TA. The WAXD patterns for the PEO/PVPh = 70/30 crystallized at 28 °C were also analyzed, as shown in Fig. 5d. For PEO/PVPh = 70/30, the relative intensity of the (032) crystal plane is also smaller than that of (120) crystal plane as observed in PEO/TA = 70/30. The same results obtained for PEO/TA = 70/30 and PEO/

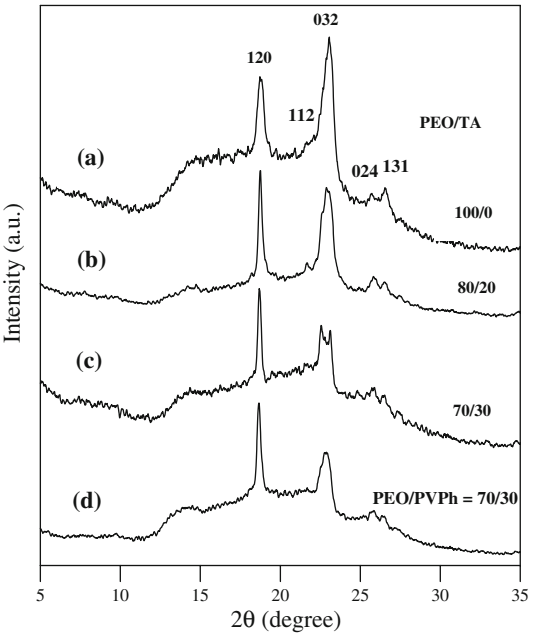

Fig. 5 WAXD patterns for PEO, PEO/TA blend, and PEO/PVPh blend cast on PI films and crystallized at 28 °C (sample film thickness was ca. 20 μm)

PVPh = 70/30 blends indicate that the change in relative intensity of the (032) crystal plane to (120) crystal plane is attributed to the strong intermolecular interaction between PEO and amorphous diluents.

Consequently, existence of the strong intermolecular interactions in PEO/TA and PEO/PVPh blends causes significant effect on the crystallographic orientation upon crystallization of PEO. The change in the crystallographic orientation in PEO in blends with another component forming strong intermolecular interactions may be the main factor for the slower growth rate of PEO. Both diffusion-limited mechanism and intrinsic characteristics can lead to formation of the dendritic morphology in PEO/TA blends.

Conclusions

Dendrites in PEO blended with TA are apparently induced and intensified by strong intermolecular H-bonding interactions, where miscibility and interactions are evident by the single and composition-dependent glass transition temperature. At TA contents increasing to 30 wt% or higher in the PEO/TA blend, the crystalline morphology of PEO undergoes a dramatic change to assume a highly dendritic form. The dendritic growth rate of PEO/TA = 70/30 shows a nonlinear relationship with respect to time due to the diffusion-limited mechanism. From the analysis of the dendritic morphology of PEO/TA = 70/30 by WAXD, the preferential crystallographic orientation is apparently more distinct in the PEO/TA = 70/30 blend, where the dendritic crystals are induced by the strong intermolecular interactions between PEO ether and TA phenol groups.

Acknowledgments The authors acknowledge the research grants from Taiwan's *National Science Council* (NSC-95 2221 E006 183).

References

1. Cheng SZD, Chen J, Janimak JJ (1990) Crystal growth of intermediate-molecular-mass poly(ethylene oxide) fractions from the melt. Polymer 31:1018–1024
2. Cheng SZD, Chen J, Barley JS, Zhang A, Habenschuss A, Zschack PR (1992) Isothermal thickening and thinning processes in low molecular-weight poly(ethylene oxide) fractions crystallized from the melt. 3. Molecular weight dependence. Macromolecules 25:1453–1460
3. Cheng SZD, Chen J, Zhang A, Barley JS, Habenschuss A, Zschack PR (1992) Isothermal thickening and thinning processes in low molecular weight poly(ethylene oxide) fractions crystallized from the melt. Polymer 3:1140–1149
4. Cheng SZD, Noid DW, Wunderlich B (1987) Molecular segregation and nucleation of poly(ethylene oxide) crystallized from the melt. IV. Computer modeling. J Polym Sci Polym Phys 27:1149–1160
5. Price C, Evans KA, Booth C (1975) Crystallization of poly(ethylene oxide) fractions: simultaneous dilatometry and calorimetry. Polymer 16:196–200
6. Shafee EE (2004) Morphology and spherulitic growth kinetics in poly(ethylene oxide)/poly(n-butyl methacrylate) blends. Polym Int 53:249–253
7. Wu L, Lisowski M, Talibuddin S, Runt J (1999) Crystallization of poly(ethylene oxide) and melt-miscible PEO blends. Macromolecules 32:1576–1581
8. Marentette JM, Brown GR (1998) The crystallization of poly(ethylene oxide) in blends with neat and plasticized poly(vinyl chloride). Polymer 39:1415–1427
9. Huang YP, Kuo JF, Woo EM (2001) Influence of molecular interactions on spherulite morphology in miscible poly(ethylene oxide)/epoxy network versus poly(ethylene oxide)/poly(4-vinyl phenol) blend. Polym Int 51:55–61
10. Huang YP, Woo EM (2001) Effects of entrapment on spherulite morphology and growth kinetics in poly(ethylene oxide)/epoxy networks. Polymer 42:6493–6502
11. Zheng H, Zheng S, Guo Q (1997) Thermosetting polymer blends of unsaturated polyester resin and poly(ethylene oxide). II. Hydrogen-bonding interaction, crystallization kinetics, and morphology. J Polym Sci Polym Chem 35:3169–3179
12. Paternostre L, Damman P, Dosiere M (1999) Morphology and crystal structure of the poly(ethylene oxide)-hydroquinone molecular complex. J Polym Sci Polym Phys 37:1197–1208
13. Reiter G (2003) Model experiments for a molecular understanding of polymer crystallization. J Polym Sci Polym Phys 41:1869–1877
14. Sommer JU, Reiter G (2000) Polymer crystallization in quasi-two dimensions. II. Kinetic models and computer simulations. J Chem Phys 112:4384–4393
15. Sommer JU, Reiter G (2005) Crystallization in ultra-thin polymer films: morphogenesis and thermodynamical aspects. Thermochim Acta 432:135–147
16. Keith HD, Padden Jr FJ (1964) Spherulitic crystallization from the melt. II. Influence of fractionation and impurity segregation on the kinetics of crystallization. J Appl Phys 35:1286–1296
17. Yen KC, Mandal TK, Woo EM (2008) Enhancement of bio-compatibility via specific interactions in polyesters modified with a bio-resourceful macromolecular ester containing polyphenol groups. J Biomed Mater Res 86A:701–712
18. Meaurio E, Zuza E, Sarasua JR (2005) Miscibility and specific interactions in blends of poly(L-lactide) with poly(vinylphenol). Macromolecules 38:1207–1215
19. Lee LT, Woo EM (2004) Miscible blends of poly(4-vinyl phenol)/poly (trimethylene terephthalate). Polym Int 53:1813–1820